PROCEEDINGS OF THE INTERNATIONAL CONFERENCE NANOMATERIALS: APPLICATIONS AND PROPERTIES
Vol. **1** No 1, 01PCN24(4pp) (2012)

Distribution and Luminescent Properties of Ce^{3+} Ions in Nanosized Calcium Hydroxyapatite

I.V. Berezovskaya, N.P. Efryushina, E.V. Zubar, V.P. Dotsenko

A.V. Bogatsky Physico-Chemical Institute, National Academy of Sciences of Ukraine, Lustdorfskaya doroga, 86, 65080 Odessa, Ukraine

(Received 19 June 2012; published online 24 August 2012)

The paper presents an analysis of the luminescent properties of Ce^{3+}-doped calcium hydroxyapatite ($Ca_{10}(PO_4)_6(OH)_2$, HAp) nanopowders prepared by the chemical precipitation and sol-gel method. It was shown that in nanoscale HAp Ce^{3+} ions are strongly perturbed by surface defects and their local symmetry differs from that of Ce^{3+} ions in the bulk crystals. Possible origin of defects in nanosized HAp is also discussed.

Keywords: Calcium hydroxyapatite, Synthesis, Nanopowders, Cerium, Luminescence.

PACS numbers: 78.47.jd; 81.07.Wx

1. INTRODUCTION

Compounds and solid solutions with the apatite-type structure are of great interest since they are used as phosphors, biomaterials and ionic exchangers. Besides, it has been recently shown that lanthanide-doped calcium hydroxyapatite (HAp) nanoparticles can be used as bioactive, fluorescent carriers of biological molecules and drugs [1,2]. HAp belongs to the hexagonal system with the $P6_3/m$ space group. In this lattice, two unequivalent calcium sites are present: Ca(I) with C_3 symmetry is surrounded by nine oxygen atoms, and Ca(II) with C_S symmetry is coordinated to six oxygen atoms and one OH^- group [3]. It is accepted that the disordering of OH^- ions in c-axis columns causes a structural complexity of HAp. It is well known that apatites can accommodate a large number of different ions in their lattice. The distribution of trivalent lanthanides (Ln^{3+}) between the two alkaline earth sites in different apatites has been the subject of numerous studies [4-7]. It has been found that trivalent lanthanides in Ca(II) position are characterized by abnormally high values of Stark splitting. This provided a distinction of the spectral features of these ions from those of Ln^{3+} in Ca(I) position. However, the results obtained are contradictory. For example, the luminescence properties of Eu^{3+} in calcium apatites under UV excitation have been studied by several authors [4,6].

It was concluded that Eu^{3+} ions occupy mainly the Ca(II) positions. In contrast to this conclusion, Karbowiak and Hubert [7] have reported that the nature of site occupancy by Eu^{3+} in calcium fluoroapatite varies depending on the material preparation method. Some of us have studied the luminescence properties of Ce^{3+} ions in $Ca_{10}(PO_4)_6(OH)_2$ prepared by solid state reaction method at 1100°C [8]. It has been found that at relatively low concentrations (≤ 0.5 at.%) Ce^{3+} ions tend to occupy preferably Ca(I) sites, and these Ce^{3+} centers cause an intense emission with maxima at 335 and 362 nm. The aim of this work is to study the influence of the preparation route on the distribution and luminescent properties of Ce^{3+} ions in HAp.

2. EXPERIMENTAL

Samples of nominal formula $Ca_{10(1-x)}Ce_{10x}(PO_4)_6(OH)_2$ (x = 0.005) used in the present work were prepared by two different methods. The samples were checked by X-ray diffraction (XRD) using Cu K_α radiation. No impurity phases were detected in the XRD patterns. Morphological investigations were carried out by scanning electron microscopy (SEM) on JEOL JSM 6390LV electron microscope. The emission and excitation spectra in UV-visible region were recorded at room temperature using a Fluorolog Fl-3 (Horiba Jobin Yvon) spectrofluorometer equipped with a xenon lamp. The measurements of emission spectra were also performed at 8 and 293 K using synchrotron radiation and the equipment of the SUPERLUMI experimental station [9] of HASYLAB (Hamburg, Germany). The Fourier-transformed infrared absorption spectra were recorded using a Bruker Vertex 70 spectrometer.

3. RESULTS AND DISCUSSION

In this work, Ce^{3+}-doped $Ca_{10}(PO_4)_6(OH)_2$ with different particle sizes have been synthesized by chemical precipitation and sol-gel method. To prepare calcium phosphate nanoparticles by a precipitation process, an aqueous solution of $(NH_4)_2HPO_4$ was slowly added to an aqueous solution of calcium nitrate tetrahydrate $Ca(NO_3)_2{\cdot}4H_2O$ upon continuous stirring. The pH of the mixture was adjusted to 10 by adding NH_4OH and the reaction temperature was maintained at 60°C. The resulting precipitate was aged for 0.5 h under stirring, and then filtered, washed with distilled water and dried at 105°C. The preparation of HAp powders by the sol-gel method [10] involved the use of aqueous solution of calcium nitrate tetrahydrate $Ca(NO_3)_2{\cdot}4H_2O$ and alcohol solution of trimethyl phosphate $(CH_3O)_3PO$ as the precursors. Some amount of citric acid (as a chelating agent) was added into aqueous solution of $Ca(NO_3)_2{\cdot}4H_2O$. The solutions were mixed at room temperature and kept at pH 7.5 for 48 h. The obtained gel was dried at 190°C for 2 h, and then fired at 600°C for 1 h. In the both cases cerium nitrate was added to the calcium nitrate solutions to obtain molar ratio of Ce/(Ca+Ce) = 0.005. The luminescent properties of the samples were analyzed in the as prepared-state and after annealing at 800°C for 2-3 h in air or in a reducing medium of CO. The average sizes of crystallites (d) of the as-prepared polycrystalline materials were calculated from XRD-patterns by the Scherrer equation [11].

The reflections from the (300) and (002) planes were used. The obtained values varied from 34 to 70 nm, in agreement with the results reported previously for HAp nanopowders prepared either by chemical precipitation method [1,12] or by the sol-gel process [10]. A typical SEM image of HAp prepared by the sol-gel method is presented in Fig. 1. It is seen that the material is composed of crystallites with an irregular form, and which exhibit a high degree of aggregation.

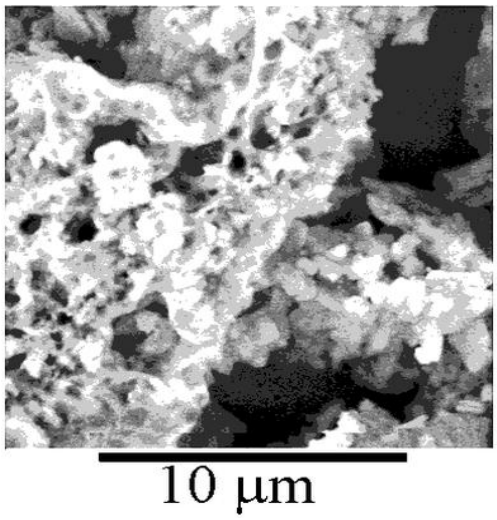

Fig. 1 – SEM photograph of $Ca_{10(1-x)}Ce_{10x}(PO_4)_6(OH)_2$ (x = 0.005) synthesized by the sol-gel method

The emission spectra of the obtained materials depend on the preparation conditions. Fig. 2 shows the emission spectra of $Ca_{10(1-x)}Ce_{10x}(PO_4)_6(OH)_2$ (x = 0.005) prepared by the chemical precipitation method. Under excitation in the 240-300 nm region, the spectrum of the as-prepared sample extends from 310 to 430 nm. It has a maximum around 370 nm and a shoulder at about 340 nm. As can be seen from Fig. 2, the annealing of this sample at 800°C significantly increases the emission intensity, and two maxima at ~ 338 nm and 368 nm are clearly observed. These changes can be attributed to the increase in the solubility of CeO_2 in HAp, and the suppression of the luminescence-quenching action produced by surface defects. One can expect that in nanoscale HAp Ce^{3+} ions in the surface region are strongly perturbed by the surface states and their point symmetry somewhat differs from that of Ce^{3+} ions in the bulk crystals.

Fig. 3 shows the low temperature time-resolved emission spectra of the $Ca_{10(1-x)}Ce_{10x}(PO_4)_6(OH)_2$ (x = 0.005) sample annealed at 800°C. Both spectra can be reasonably decomposed into three Gaussian-type bands peaked at 335, 362 and 388 nm. Their origin has been discussed previously by some of us [8]. The bands at 335 and 362 nm must be attributed to the transitions from the lowest Ce^{3+} 5d excited state to the 4f ground state levels $^2F_{5/2}$ and $^2F_{7/2}$. The energy gap between the maxima (1960 cm^{-1}) coincides with the spin-orbit splitting of Ce^{3+} ground state.

We will denote all the centers related to the 335 and 362 nm emission bands as Ce_I. It is clear that the spectra in Figs. 2,3 are mainly due to the Ce_I emission. The centers related to the 388 nm emission band will be denoted as Ce_{II}. Note that the Ce_{II} emission band does not show its characteristic doublet structure, indicating that there are several Ce^{3+} centers with overlapping spectra.

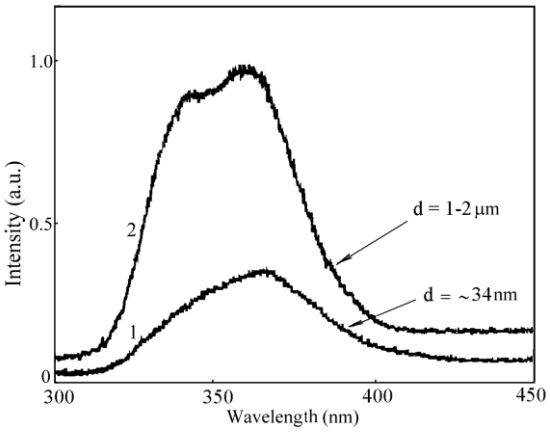

Fig. 2 – The emission spectra of $Ca_{10(1-x)}Ce_{10x}(PO_4)_6(OH)_2$ (x = 0.005) prepared by the chemical precipitation method: 1- as-prepared sample; 2- after firing at 800°C for 2 h in air. The spectra were recorded at 293 K upon excitation at 266 nm

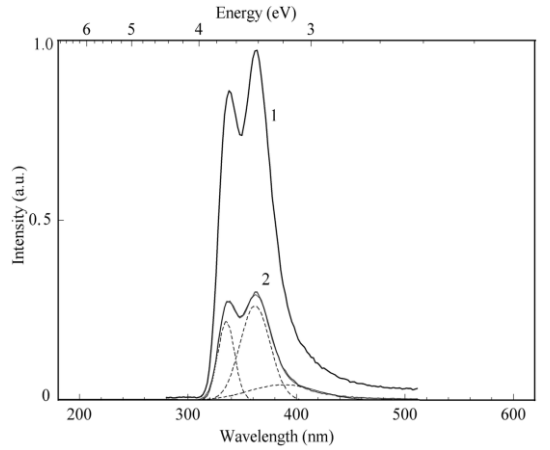

Fig. 3 – The time-resolved emission spectra of the $Ca_{10(1-x)}Ce_{10x}(PO_4)_6(OH)_2$ (x = 0.005) sample at 8 K (λ_{exc} = 266 nm). The spectra were recorded for two different time intervals (Δt) after picosecond pulse excitation: (1) Δt = 1-190 ns; (2) Δt = 1-8 ns

It was shown that the dominant center (Ce_I) with emission maxima at 335 and 362 nm consists of a Ce^{3+} ion in the Ca(I) position [8]. In this case, the charge compensation for Ce^{3+} ions is provided by calcium vacancies, and in samples with relatively high concentrations of Ce^{3+}, a single calcium vacancy will compensate one Ce^{3+} ion distantly and one Ce^{3+} locally.

The other type of Ce^{3+} centers (Ce_{II}) can be attributed to a Ce^{3+} ion on the Ca(II) position. The charge compensation of Ce^{3+} ions occupying the Ca(II) positions is provided by substitution of OH^- ions by O^{2-}. This mechanism implies the formation of the neutral $(Ce_{Ca}^{\bullet}O_{OH})^{\times}$ associates. This causes the lower-energy position of the Ce_{II} emission band (~390 nm) as compared to the Ce_I emission band due to a larger crystal field splitting of the Ce^{3+} 5d configuration and to strengthening of the covalent bond between Ce^{3+} and its environment.

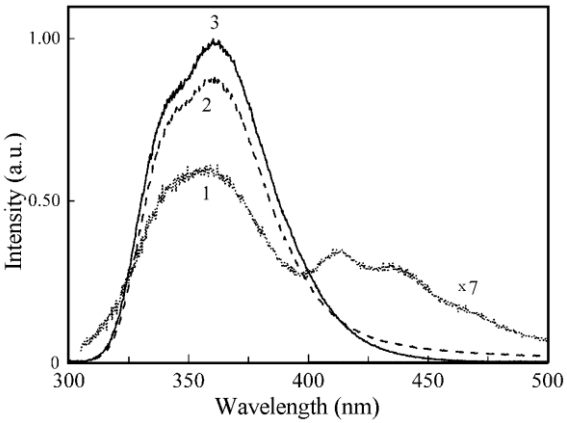

Fig. 4 – The emission spectra of $Ca_{10(1-x)}Ce_{10x}(PO_4)_6(OH)_2$ (x = 0.005) prepared by the sol-gel method: 1 - as-prepared sample; 2- after firing at 800°C for 3 h in a reducing medium of CO; 3 - after firing at 800°C for 3 h in air. The spectra were recorded at 293 K upon excitation at 288 nm

The emission spectra of $Ca_{10(1-x)}Ce_{10x}(PO_4)_6(OH)_2$ (x = 0.005) prepared by the sol-gel method are presented in Fig. 4. The emission spectrum of the as-prepared sample extends from 300 to 500 nm and has a local maximum around 360 nm, which can be attributed to the Ce^{3+} 5d → 4f transitions. In addition to the Ce^{3+} 5d → 4f emission band the spectrum contains relatively intense features at 414 and 434 nm. It is seen that the annealing of the sample at 800°C suppresses completely the emission in the 400-460 nm region, whereas the high energy band shows clearly the doublet structure and its intensity increases significantly. The positions of the maxima (335 and 362 nm) are in agreement with those found for the Ce_I emission in HAp prepared either by the chemical precipitation method (see Fig. 2) or by solid state reactions [8].

The results presented in Fig. 4 indicate that the emission in the 410-500 nm range is not an intrinsic property of HAp, but is due to unknown defects or impurities. The probable candidates are CO_2^- radicals situated in numerous pores of the nanosized HAp. Indeed, Zhang et al. [13] have revealed that strontium hydroxyapatite microspheres prepared by facile solvothermal process exhibit an intense broadband emission with a maximum at 427 nm. This emission was tentatively assigned to the CO_2^- radicals formed during the synthesis process. Earlier, Angelov et al. [14] have reported that the CO_2^- radicals in interstitial positions of the aragonite lattice are probably responsible for self-activated luminescence around 490 nm in $SrCO_3$. This interpretation is indirectly supported by the following experimental facts: a) defects responsible for the emission at 414 and 434 nm are not stable at 800°C (see Fig. 4), b) $Ca_{10(1-x)}Ce_{10x}(PO_4)_6(OH)_2$ (x = 0.005) prepared by the sol-gel method contains significant quantity of carbonate ions (CO_3^{2-}). Fig. 5 shows the typical FTIR absorption spectrum of HAp prepared by the sol-gel method. It contains the stretching and bending vibration bands of OH^- groups at 3572 and 631 cm^{-1}, asymmeric (ν_3) and symmetric (ν_1) stretching vibration bands of the isolated PO_4^{3-} groups at 1090, 1039 and 960 cm^{-1}.

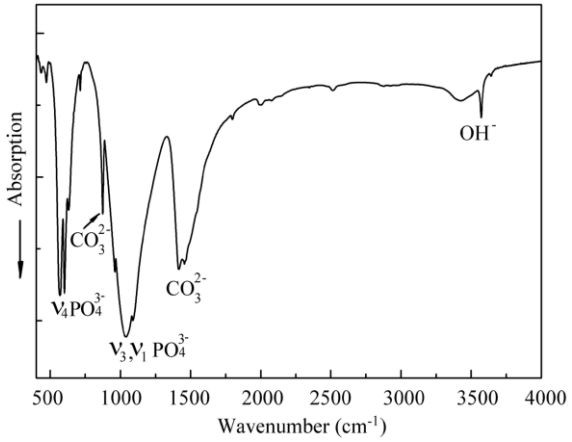

Fig. 5 – FTIR absorption spectrum of HAp prepared by the sol-gel method

The bending vibrations (ν_4, ν_2) of the PO_4^{3-} groups cause the bands at 601, 568 cm^{-1} and 472 and 435 cm^{-1}, respectively. In addition to these features, there are bands at 1457, 1416 and 873 cm^{-1}, which must be attributed to the stretching and bending vibrations of the CO_3^{2-} anions occupying both the OH^- and PO_4^{3-} positions [10,12,15]. Since these bands were absent in FTIR absorption spectrum of HAp prepared by the chemical precipitation method, one can expect that the incorporation of the CO_3^{2-} groups into the crystal lattice is a consequence of the use of citric acid as a reagent. It is evident that this can be also responsible for the presence of CO_2^- radicals in HAp prepared by the sol-gel method.

4. CONCLUSIONS

Ce^{3+}-doped $Ca_{10}(PO_4)_6(OH)_2$ with different particle sizes have been synthesized by the chemical precipitation and sol-gel method. The site preference of Ce^{3+} ions for the two calcium sites Ca(I), Ca(II) in the apatite structure was studied by means of luminescent spectroscopy. It was found that the distribution of Ce^{3+} ions on the calcium sites depends on the preparation conditions. Although Ce^{3+} ions tend to occupy the Ca(I) positions with C_3 symmetry in nanoscale HAp they are strongly perturbed by different surface defects, so that their local symmetry differs from that of Ln^{3+} ions in the bulk crystals.

REFERENCES

1. S.P. Mondejar, A. Kovtun, M. Epple, *J. Mater. Chem.* **17**, 4153 (2007).
2. P. Yang, Z. Quan, C. Li, X. Kang, H. Lian, J. Lin, *Biomaterials* **29**, 4341 (2008).
3. J.M. Hughes, M. Cameron, A. Mariano, *Amer. Mineral.* **76**, 1165 (1991).
4. R. Jahannathan, M. Kottaisamy, *J. Phys.: Condens. Matter.* **7**, 8453 (1995).
5. A. Serret, M.V. Cabanas, M. Vallet-Regi, *Chem. Mater.* **12**, 3836 (2000).
6. R. Sahoo, S.K. Bhattacharya, R. Debnath, *J. Sol. State Chem.* **175**, 218 (2003).

7. M. Karbowiak, S. Hubert, *J. Alloys Compd.* **302**, 87 (2000).
8. I.V. Berezovskaya, N.P. Efryushina, G.B. Stryganyuk, A.S. Voloshinovskii, E.V. Zubar, V.P. Dotsenko, *Func. Mater.* **15**, 164 (2008).
9. G. Zimmerer, *Radiat. Meas.* **42**, 859 (2007).
10. C.L. Chu, P.H. Lin, S. Dong, D.Y. Guo, *J. Mater. Sci. Lett.* **21**, 1793 (2002).
11. H.P. Klug, L.E. Alexander, *X-ray diffraction procedures for polycrystalline and amorphous materials* (New York: Willey-Interscience: 1974).
12. L.M. Rodriguez-Lorenzo, M. Vallet-Regi, *Chem. Mater.* **12**, 2460 (2000).
13. C. Zhang, Z. Cheng, P. Yang, Z. Xu, C. Peng, G. Li, J. Lin, *Langmuir* **25**, 13591 (2009).
14. S. Angelov, R. Stoyanova, R. Dafinova, K. Kabasanov, *J. Phys. Chem. Solids* **47**, 409 (1986).
15. I.R. Gibson, I. Rehman, S.M. Best, W. Bonfield, *J. Mater. Sci. Mater. Med.* **12**, 799 (2000).